

Ozone loss in the Arctic polar vortex inferred from high-altitude aircraft measurements

M. H. Proffitt^{*}, J. J. Margitan[†], K. K. Kelly[‡], M. Loewenstein[§], J. R. Podolske[§] & K. R. Chan[§]

^{*} NOAA Aeronomy Lab, 325 Broadway, Boulder, Colorado 80303 and CIRES, University of Colorado, Boulder, Colorado 80309, USA

[†] Jet Propulsion Laboratory, California Institute of Technology, Pasadena, California 91109, USA

[‡] NOAA Aeronomy Lab, 325 Broadway, Boulder, Colorado 80303, USA

[§] NASA Ames Research Center, Moffett Field, California 94035, USA

The Arctic polar vortex in winter is known to be chemically primed for ozone depletion, yet it does not exhibit the large seasonal ozone decrease that characterizes its southern counterpart. This difference may be due in part to a net flux of ozone-rich air through the Arctic vortex, which can mask ozone loss. But by using a chemically conserved tracer as a reference, significant ozone loss can be identified. This loss is found to be correlated with high levels of chlorine monoxide, suggesting that much of the decrease in ozone is caused by anthropogenic emissions of chlorofluorocarbons.

IN 1985 Farman *et al.*¹ reported that spring values of total column ozone over Halley Bay, Antarctica, had decreased considerably during the previous decade, and they suggested that certain chlorine-containing compounds could be causing the observed ozone depletion. Further studies have supported these findings²⁻⁵ and refined understanding of high-latitude ozone loss.

During the 1987 Airborne Antarctic Ozone Experiment (AAOE)⁵ *in situ* measurements of many chemical species and meteorological parameters were made from a NASA high-altitude aircraft (ER-2) on twelve flights out of Punta Arenas, Chile (53° S), at cruise altitudes of ~17–19 km. *In situ* measurements of ozone (O₃)⁶, nitrous oxide (N₂O—a chemically conserved tracer)⁷, chlorine monoxide (ClO)⁸, temperature, pressure and wind speed⁹ were made.

Potential temperature (Θ) is a measure of entropy and is calculated from measured pressure and temperature. In the absence of diabatic processes, parcels tend to move on constant Θ surfaces and mix with other parcels on that surface. Because Θ increases with altitude, and air movement is stratified somewhat by Θ , we use it here in place of altitude as a vertical coordinate. Using Θ , diabatic processes (net heating or cooling) can be more easily identified. The aircraft flights were usually to 72° S on surfaces of constant Θ (isentropic). AAOE lasted from 17 August to 22 September, covering late winter and early spring in the Southern Hemisphere. It was found that the O₃ mixing ratio at 72° S decreased by 61% at $\Theta = 425$ K (17 km) over a 30-day period⁶ and was precisely collocated with very high ClO mixing ratios¹⁰. Calculations indicated that the observed concentration of ClO was high enough to link the O₃ decrease to catalytic destruction by chlorine¹¹⁻¹³. These calculations, however, included two important assumptions: that diabatic cooling was negligible and that the vortex air was not being replenished by O₃-rich air from outside the polar jet. This view of the polar jet as a 'containment vessel' is supported in the analyses of some authors^{1,14-16} but not by others¹⁷⁻²².

Possible Arctic ozone loss has also been reported recently. Balloon data taken during 1989 suggest that ozone depletion occurred late in January at an altitude of 22–26 km over Kiruna,

Sweden (68° N)²³, and that there was a depleted ozone layer from 18 to 24 km from 24 January to 22 February over Alert, Canada (82° N)²⁴. Another indication of possible ozone loss in the Arctic winter was found by the Ozone Trends Panel²⁵, where a comparison of total column ozone data from 1979–80 with 1986–87 shows a decrease of 4–10% between 65° and 80° N during the period from November to February.

An aircraft campaign, similar to AAOE, the Airborne Arctic Stratospheric Expedition (AASE) was based at Stavanger, Norway (59° N) from 3 January to 10 February 1989, to study ozone destruction mechanisms during the Arctic mid-winter²⁶. The instrumentation used on the 14 ER-2 flights was virtually identical to that used in the Antarctic, but the aircraft flew nearer the pole in the Arctic, usually to 79° N. Although the Antarctic vortex persists well into spring, the less stable Arctic vortex usually dissipates in late winter and so the Arctic measurement campaign had to be conducted earlier in the season. Large photochemical ozone loss was not expected during this period of minimum solar radiation and, as anticipated, no large isentropic temporal decrease in ozone was found in the Arctic.

The analysis we present is based on a moving coordinate system defined vertically by Θ and horizontally by latitude referenced to the vortex boundary, which was defined as the latitude of peak wind speed as measured from the aircraft. The average latitude of the boundary is 68° N with a standard deviation of 3°. For the analysis that follows, the data will be considered in three regions: the vortex exterior (from aircraft take-off at 59° N to the boundary), the outer vortex (the first 8° of latitude inside the vortex boundary, comprising about 60% of the vortex volume) and the inner vortex (the remainder of the vortex, usually including the pole). The outer vortex receives more solar radiation than the inner vortex, and so photochemical ozone loss is more likely to occur there.

An analysis similar to that used to show that there is ozone loss outside the Antarctic ozone hole²⁷ will be used to show that there is also significant ozone loss in the Arctic vortex. Fundamental to the arguments presented is that standard gas-phase photochemistry identifies the primary source region for O₃ and the loss region for N₂O as the tropical middle stratosphere and also predicts long photochemical lifetimes for N₂O and O₃ (more than a year) for high-latitude winter²⁸⁻³¹. From this, we deduce that air parcels at high latitudes with the same N₂O mixing ratios should have very similar O₃ mixing ratios. Deviations from this behaviour thus indicate chemical ozone loss occurring by processes not included in standard gas-phase photochemistry models³².

In the following section, O₃ and N₂O data are presented and their relative behaviour during the mission characterized. In the section that follows, we argue that the vortex behaves as a 'flowing processor' and these data are evaluated in this context, and an apparent O₃ loss is identified within the vortex. The origin of the loss is shown to be chemical rather than dynamical, to be enhanced in the outer vortex, and to have occurred both during and before the mission. The O₃ and N₂O data taken outside the vortex where O₃ loss is expected to be small are compared with values found within the vortex where an O₃ loss

is identified. The loss in the outer vortex is linked with high concentrations of ClO.

O₃ and N₂O at high latitudes

There are insufficient simultaneous measurements of lower stratospheric O₃ and N₂O available to determine an accurate climatology for these trace species, and so our analysis relies solely on the measurements made during AASE. An example of mid-latitude N₂O and O₃ data is given in Fig. 1*a*. These data are from an AASE transit flight on 21 February 1989 at 37–39° N latitude. A nearly linear relationship between O₃ and N₂O can be seen. Although the data only include N₂O values down to 165 parts per 10⁹ by volume (p.p.b.v.), the fit to the data agrees well with the linear fit to observations taken by the ATMOS (Atmospheric Trace Molecule Spectroscopy) instrument³³ during May 1985 at 28° N and 48° S from Spacelab 3. The linear

fit to ATMOS data shown in Fig. 1*a* includes all data with N₂O > 50 p.p.b.v., and extends the range of the linear relation, seen in the AASE data. The potential temperature, Θ , of each data point is indicated by colour and symbol type. As is typical of the lower stratosphere (altitude < 25 km), O₃ increases with altitude (increasing Θ) whereas N₂O decreases. At mid-latitudes, O₃ peaks typically above 30 km and then decreases, but N₂O continues to decrease with increasing altitude. Maximum O₃ mixing ratios at high latitudes are between 25 and 30 km, about 5–10 km above ER-2 altitudes^{23,24}.

Figure 1*b* represents all data with $\Theta > 400$ K taken in the vortex exterior. Also shown are linear fits to each of the Θ bins. Except at the lowest Θ , these data are very similar to those found in Fig. 1*a*, but with greater variability, and with lower values of O₃ relative to N₂O. The plot in Fig. 1*c* shows all the AASE data with $\Theta > 400$ K that are in the outer vortex. A linear

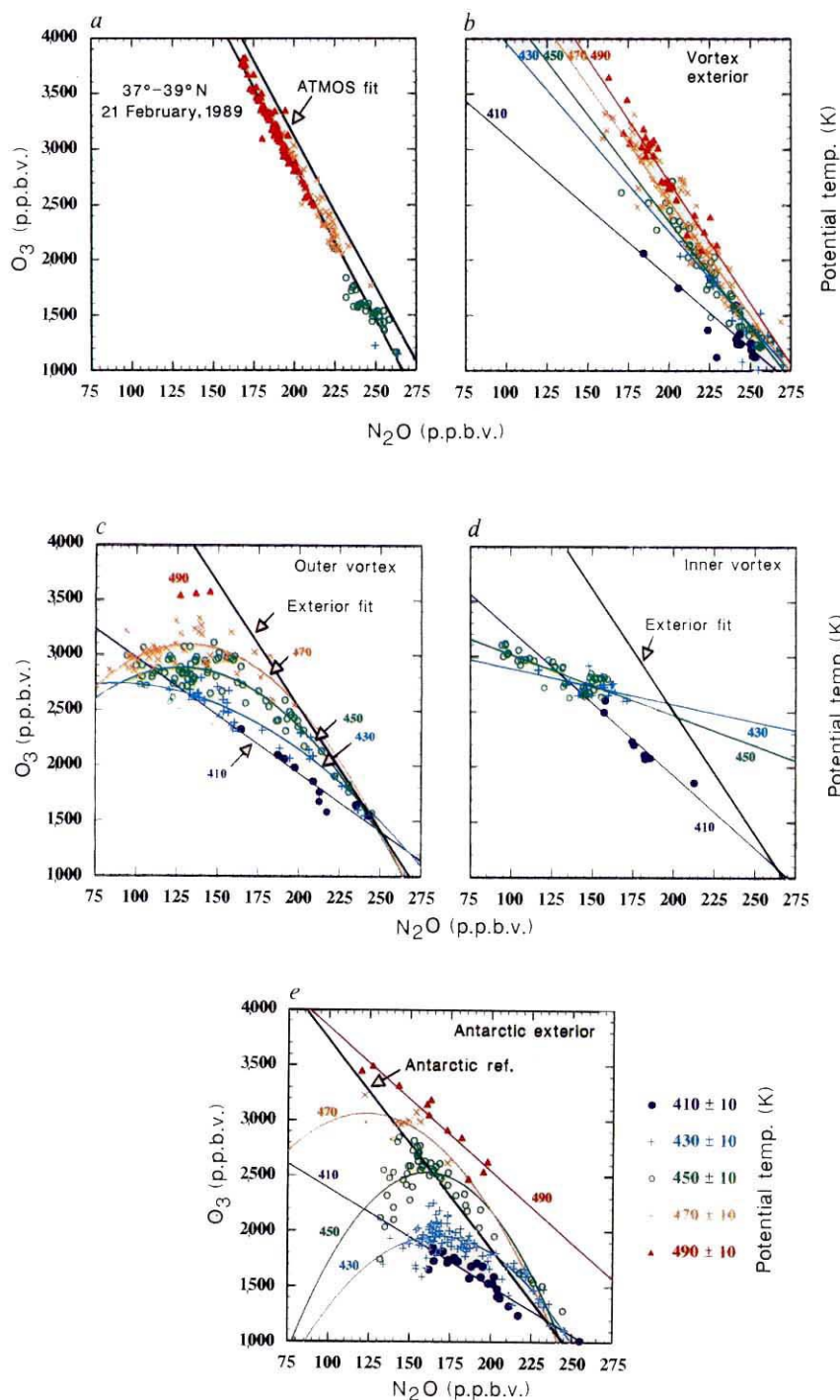
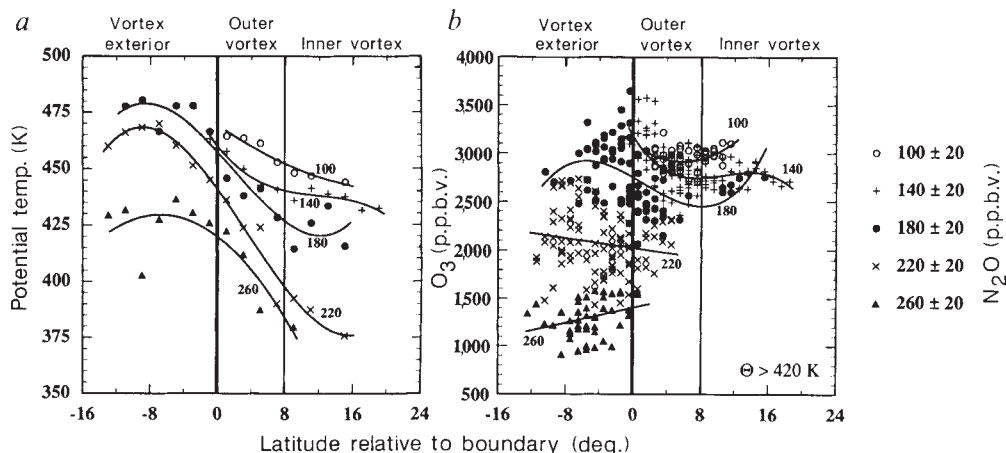


FIG. 1 O₃ is plotted against N₂O and colour coded for Θ . *a*, Data from 21 February 1989 at 37–39° N latitude averaged for 100 s (about 10' of latitude) and a linear fit to that data. Also shown is linear fit to ATMOS data taken from Spacelab 3 at 28° S and 40° N latitude in May 1985. *b*, All AASE data taken in vortex exterior (59° N to vortex boundary) with $\Theta > 400$ K, and averaged for each flight leg over 1° of latitude relative to the boundary of the vortex. Fits to data are provided for Θ bins and are discussed in the text. *c*, Same as (*b*) except that the data are from the outer vortex (the first 8° of latitude inside vortex boundary). *d*, Same as (*b*) except that the data are from the inner vortex (all of vortex interior more than 8° of latitude inside the vortex boundary). *e*, Same as (*b*) except the data are from the exterior of the Antarctic vortex during AAOE (1987).

FIG. 2 *a*, N_2O isopleths on a coordinate system of Θ plotted against latitude relative to the boundary of the vortex. Data from the entire mission are averaged over 1° of latitude relative to the vortex boundary and plotted along with polynomial fits for each of the N_2O bins. *b*, All O_3 data with $\Theta > 420$ K are plotted against latitude relative to the boundary and binned by N_2O . Data are averages over 100-s intervals (about $10'$ of latitude). A fit is provided for each bin.



fit is shown for the 410 K bin with quadratic fits for the three middle bins. The highest bin (490 K) has too few data to justify a fit. Figure 1*d* shows data from the inner vortex. Comparing Fig. 1*b-d*, the fits for the 410 K bin are all very similar, but there is little similarity in the fits to the other Θ bins. The uniformity below 420 K indicates that air is free to move from inside to outside the vortex at this level, suggesting that the 'bottom of the vortex' is where $\Theta = 410 \pm 10$ K.

Another important criterion for comparing Fig. 1*b-d*, and indicative of chemical loss of O_3 , is the deviation of O_3 mixing ratios relative to N_2O from the mid-latitude values shown in Fig. 1*a*. It is clear that for a constant value of N_2O , O_3 progressively decreases from the mid-latitudes, to the vortex exterior, to the outer vortex. In Fig. 1*b, c*, O_3 also decreases with decreasing Θ . The characteristic of decreasing O_3 with decreasing Θ for a constant value of N_2O will be referred to as ' O_3 - Θ dependence'. There is a small O_3 - Θ dependence in the vortex exterior and a larger one in the outer vortex, but none is evident in the mid-latitude data, nor in the inner vortex. The O_3 - Θ dependence in Fig. 1*b, c* is not a result of downward mixing of air from above the O_3 maximum because O_3 and Θ are negatively correlated above the maximum, whereas the O_3 - Θ dependence in Fig. 1*b, c* is positive. This implies that the O_3 - Θ dependence is not a result of dynamics, but of chemistry.

This O_3 - Θ dependence was also clearly seen in the Antarctic exterior (Fig. 1*e*) and seems much like the Arctic outer vortex (Fig. 1*c*). Also given in Fig. 1*e* is the Antarctic reference that was used for assessing O_3 loss²⁷. That reference was based on a more restricted data set than is available for the Arctic, and may underestimate O_3 loss because it was chosen very conservatively.

Isopleths for N_2O (lines of constant N_2O) within our Θ -latitude coordinate system are shown in Fig. 2*a*. Each point is

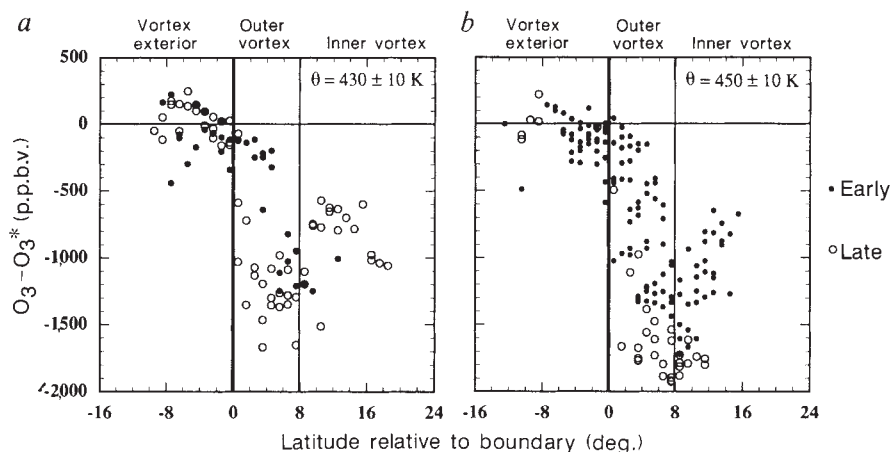
an average over 1° of latitude and over all flights of the mission. Polynomial fits are provided for each of the N_2O bins and are good approximations to the N_2O isopleths. The poleward decrease in Θ along the isopleths indicates diabatic cooling within the vortex. Diabatic cooling rates during the mission have been approximated theoretically³⁴ and from AASE N_2O data³⁵. Although these analyses do not necessarily represent average vortex conditions, they do imply that cooling of at least 0.9 K per day in Θ (0.4 K per day in temperature) occurred during the mission both inside and outside the vortex.

Figure 2*b* confirms the O_3 loss seen in Fig. 1*a-d* but in a spatial context, by plotting O_3 against latitude relative to the vortex boundary for the same five N_2O bins of Fig. 2*a*. Only data above 420 K are plotted, to exclude data that may be affected by the relatively unrestricted horizontal exchange of air at the bottom of the vortex. Again polynomial fits are included for each of the N_2O bins and terminated where the data end. In the outer vortex, O_3 decreases towards the pole, and where there are data within the inner vortex, the fits there either increase or flatten out indicating less ozone loss. The outer vortex receives more solar radiation, and so the observed spatially enhanced decrease is consistent with O_3 being photochemically destroyed.

O_3 loss in a flowing processor

Early research indicated that tropospheric air enters the lower stratosphere in the tropics and exits at higher latitudes^{36,37} and this is still generally accepted³⁰. That is, the dominant atmospheric circulation is upward at low latitudes where heating lifts air into the region of the stratosphere where ozone is produced, then poleward and at high latitudes downward, due to diabatic cooling. As previously mentioned, some authors believe that the Antarctic jet effectively terminates the poleward component, but only the question of Arctic containment will be discussed here.

FIG. 3 $O_3 - O_3^*$ plotted against latitude relative to the vortex boundary for the early data (before 30 January) and the late data (the remainder of the mission), each point representing, from a flight leg, the average over 1° of latitude relative to the boundary. Negative values indicate loss of O_3 relative to the vortex exterior. *a*, Includes only those points with $\Theta = 430 \pm 10$ K. *b*, Includes only those points with $\Theta = 450 \pm 10$ K.



It has been shown that total column O_3 substantially increases at polar latitudes in the Northern Hemisphere throughout the winter months³⁸⁻⁴⁰. Because O_3 is not created at high latitudes during the winter, any increase in column O_3 must be a result of poleward flux. A recent comprehensive analysis⁴¹ shows that the meridionally averaged O_3 column at polar latitudes increases by 40 to 70 Dobson Units (DU) per month from December to February, corresponding to column changes of about 12–20% per month. With regard to 1989, satellite total column data show an increase of about 15% in the outer vortex during the mission, and an increase of more than 15% is evident from 11 column measurements and 19 balloon soundings taken from 10 January to 8 February at 82° N (ref. 42). The column increase can only be explained by a poleward flux of mid-latitude air that carries more O_3 into the polar vortex than is removed by dynamical or chemical processes. We deduce therefore, both from the Arctic long-term record and analysis of 1989 data, that the vortex is not isolated, although the Arctic polar jet may restrict poleward flux.

A more difficult question to answer that is somewhat controversial is 'At what altitudes does significant mass enter the Arctic vortex?'. Leovy *et al.*⁴³ argue that diabatic descent within the vortex, along with major and minor stratospheric warming events in the middle stratosphere, account for the polar column increase, and Kent *et al.*⁴⁴ use aerosol extinction measurements to indicate that mass flow into the vortex is somewhat restricted at its boundary. These analyses may seem to imply, but they do not conclusively show, that the polar jet completely isolates the vortex in the lower stratosphere. For consider the following: (1) The analysis of Leovy *et al.* indicates that only one-third of the total column O_3 increase occurred above 30 mbar (~23 km). (2) Kent *et al.* infer from vertical mass-flux rates near the pole that the flux into the vortex between 14 and 24 km is approximately

equal to the downward flux within the vortex from above 24 km. (3) Only 20–25% of the Arctic winter O_3 column is above 25 km and 12–20% column increases occur each winter month. This implies that a mass of O_3 equivalent to its column above 25 km must be added to the column within the vortex every 1–2 months, plus an additional amount to balance any flow out of the bottom of the vortex. Furthermore, if (2) is accurate, then the column increase below 23 km from (1) could result primarily from O_3 flux into the vortex in the lower stratosphere rather than from vertical descent. This flux could occur during warming events⁴³ (isentropic) or from diabatic circulation into the vortex. The qualitative arguments that follow do not generally rely on either of these positions, but the arguments involved in quantifying O_3 loss do.

Searching for a possible explanation for the O_3 - Θ dependence that is consistent with Fig. 1a-d and does not require a large winter O_3 loss, we consider that the loss may have occurred before winter. Theoretical and experimental evidence for a net O_3 loss over Antarctica during the continuous daylight of the summer has been presented by Farman *et al.*⁴⁵. The authors report that the loss is not primarily due to chlorine but to low concentrations of N_2O_5 and an associated enhancement of the NO_x catalytic cycle in the middle stratosphere. These loss mechanisms apply as well to the Arctic. For the summertime loss to affect our wintertime analysis requires that a substantial part of the depleted lower-stratospheric air remains at high latitudes until the polar vortex has formed in November, and is then contained at polar latitudes until the end of the mission in February. Diabatic cooling during the winter without concurrent O_3 loss implies an isentropic O_3 increase (because O_3 increases with Θ), but this was not observed. Therefore the O_3 - Θ dependence is not simply a residual of summertime loss, but must reflect wintertime loss. Furthermore, the O_3 climatology

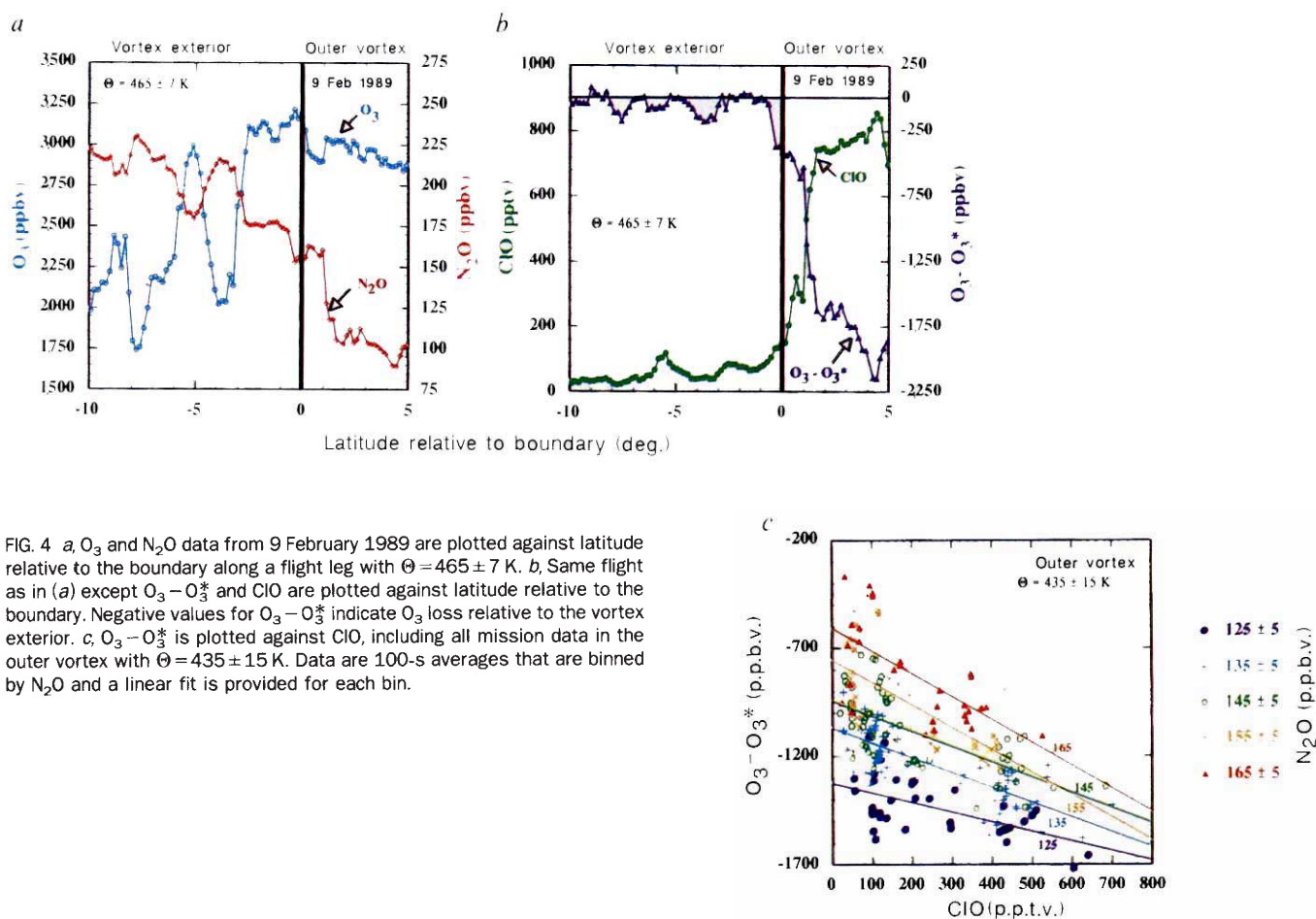


FIG. 4 a, O_3 and N_2O data from 9 February 1989 are plotted against latitude relative to the boundary along a flight leg with $\Theta = 465 \pm 7$ K. b, Same flight as in (a) except $O_3 - O_3^*$ and ClO are plotted against latitude relative to the boundary. Negative values for $O_3 - O_3^*$ indicate O_3 loss relative to the vortex exterior. c, $O_3 - O_3^*$ is plotted against ClO, including all mission data in the outer vortex with $\Theta = 435 \pm 15$ K. Data are 100-s averages that are binned by N_2O and a linear fit is provided for each bin.

discussed earlier⁴¹ shows a column increase of 12–20% per month from December to February, but also shows that the column decrease reaches a maximum in May at 12% per month, decreasing almost linearly to no change in October. Assuming the column loss in summer is representative of chemical O₃ loss, we conclude that a summer loss of O₃, terminating months before AASE, is not likely to contribute substantially to the loss reported here. But to quantify its possible effect requires very accurate O₃ and N₂O data measured simultaneously throughout the polar lower stratosphere in autumn and winter, and no such data are available.

Returning to the O₃– Θ dependence, a plausible explanation for the low O₃ and its dependence on Θ can be constructed in the context of a ‘flowing processor’. First, recall that air is diabatically cooling both inside and outside the vortex, that N₂O is chemically inert in the high latitude winter, and that mixing ratios do not change due to expansion and contraction. Therefore, if mixing of air parcels of differing N₂O content is ignored, the movement of a parcel that is diabatically cooling must be restricted to a surface described by the N₂O isopleth on which that parcel resides. This can be visualized with or without containment of the lower vortex. Consider an air parcel initially a few degrees of latitude outside the vortex that is diabatically cooling. The parcel remains on a surface of constant N₂O, so as Θ decreases, the parcel moves poleward and downward into the vortex (see Fig. 2a) thus describing a ‘flow’ into the vortex in the lower stratosphere. Alternatively, if the lower vortex is assumed to be contained by the polar jet, the cooling would be characterized as a change in N₂O on a surface of constant potential temperature, Θ (ref. 35). In this case the flow is vertical and downward as the isopleths sink. But in both cases, there is flow through the surfaces of constant Θ within the vortex in the lower stratosphere.

Let us hypothesize that by some chemical ‘process’, as an air parcel diabatically cools, O₃ is lost, and see if the resulting ‘flowing processor’ would produce the observed data. Figure 2b shows O₃ decreasing poleward along the N₂O isopleths, in the outer vortex, but not in the inner vortex. That is, the O₃ loss seems to be less in the inner vortex. Therefore our cooling/O₃-loss hypothesis, together with an enhanced loss in the outer vortex (where there is greater solar radiation), is consistent with Fig. 2, with or without mass flux into the lower vortex.

Similar reasoning can also be applied to Fig. 1b–d to again test our expanded hypothesis, this time assuming that there is mass flux into the lower vortex. Consider an air parcel with, for example, N₂O = 175 p.p.b.v. originally outside the boundary at $\Theta = 470$ K and O₃ = 3,050 p.p.b.v. (Fig. 1b). Later that parcel contains only 2,400 p.p.b.v. of O₃ when $\Theta = 430$ K inside the boundary (Fig. 1c), representing a 20% O₃ loss. But the inner vortex O₃ at 430 K is 2,700 p.p.b.v. and, as previously noted, shows no O₃– Θ dependence (Fig. 1d). Again, these data indicate that increased exposure to solar radiation in the outer vortex enhances the O₃ loss. The lack of O₃– Θ dependence in the inner vortex could be a result of enhanced isentropic mixing in that region and the low O₃ may be due to transport from the outer vortex where the loss is primarily occurring. The summertime O₃ loss discussed earlier could also explain part of the inner vortex loss.

As discussed above, air parcels at high latitudes with the same N₂O mixing ratios would be expected to have very similar wintertime O₃ mixing ratios. This was deduced without requiring the somewhat controversial assumption of significant mass flux into the vortex in the lower stratosphere. How accurately we can quantify O₃ loss from N₂O depends on how well the O₃ and N₂O reference relationship is known, and this is related to the altitude of mass flux. That is, a significant flux across the boundary at or near flight altitudes implies that air sampled inside the boundary recently entered the vortex, carrying with it the measured characteristics of the exterior. A path higher in the stratosphere requires the assumption that the O₃–N₂O refer-

ence relationship is preserved at altitudes above the region sampled by the aircraft, and therefore implies greater uncertainty in the amount of O₃ loss. Figure 1a supports this assumption.

To quantify O₃ loss within the vortex, a linear least-squares fit to all the exterior data (Fig. 1b) is calculated, excluding those points at the bottom of the vortex where $\Theta < 420$ K. This fit is shown in Fig. 1c, d and is given by

$$O_3^*(\text{p.p.b.v.}) = 7,019 - 22.42 \times N_2O (\text{p.p.b.v.})$$

where O₃^{*} approximates the O₃ mixing ratio in the vortex exterior from the mixing ratio of N₂O. For any sampled parcel inside the vortex, O₃^{*} can be calculated from its N₂O content with a negative value for O₃ – O₃^{*} representing loss relative to the vortex exterior. The mid-latitude O₃–N₂O fit (Fig. 1a) is not used as a reference, instead we use the data in the vortex exterior for the comparison. For the reasons discussed in this section, O₃ – O₃^{*} may overestimate O₃ loss within the vortex.

Figure 3 shows O₃ – O₃^{*} plotted against latitude relative to the vortex boundary for $\Theta = 430 \pm 10$ K and 450 ± 10 K. Loss in excess of 1,500 p.p.b.v. is found in the outer vortex with about two-thirds of that loss in the inner vortex. The data are also binned into early (before 30 January) and late data (the remainder). There are small temporal changes seen in the outer vortex, although Fig. 3a includes virtually no data from the first half of January because early flight legs were above $\Theta = 440$ K. Temporal changes are better represented in Fig. 3b, showing a decrease of ~ 500 p.p.b.v. This isentropic decrease in O₃ is a result of the temporal changes in N₂O, not absolute O₃ changes. Therefore, isentropic temporal analysis of O₃ alone will not reveal the true temporal decrease.

An O₃ decrease of 13 ± 8 p.p.b.v. per day has been reported by others³⁵ also using AASE data. The analysis was restricted to a few vertical profiles within the vortex and required a diabatic cooling rate estimated from N₂O and an assumption of strictly vertical descent. If the same cooling rates (0.9 K per day in Θ) are applied to the fits in Fig. 1c and no account is made for O₃ flux into the vortex, loss rates of from 9 p.p.b.v. per day where N₂O = 210 p.p.b.v. to 24 p.p.b.v. per day where N₂O = 130 p.p.b.v. are obtained.

As O₃ is low within the vortex early in the mission, a result of O₃ flux from above or from the exterior of the vortex without concurrent O₃ loss would be increased O₃ relative to N₂O; that is, the interior O₃–N₂O relationship would appear increasingly similar to the exterior relationship. This was not observed, again implying, as found in the discussion on summertime loss, that O₃ was chemically destroyed during the mission. From Fig. 3, O₃ loss had occurred by January. Further analysis of individual flights reveals that, on the first flight, 3 January, $\sim 1,000$ p.p.b.v. of O₃ had been lost at 465 K; that is, substantial O₃ loss had occurred before the mission.

Our analysis of the flowing processor still leaves an important question unanswered: ‘What is the cause of the O₃ loss?’. As previously mentioned, the cause of the Antarctic O₃ loss has been attributed to catalytic destruction by chlorine, and, to a lesser degree, bromine. Model calculations for the Arctic based on measured ClO and BrO suggest that O₃ loss approached 12% (about 12 p.p.b.v. per day) during the Arctic campaign⁴⁶. Coupled photochemical–microphysical lagrangian model calculations indicate that an O₃ loss of more than 20 p.p.b.v. per day could have been sustained throughout much of February⁴⁷. Solar radiation and measured ClO increased substantially during the mission⁴⁸, so losses should be much less in early January. Therefore, the loss indicated in our analysis for early January is too large to match these model studies. But meteorological data show that temperatures were low enough to form polar stratospheric clouds at 30 mbar by late November (A. F. Tuck, personal communication), and the eccentricity of the Arctic vortex is sufficient to frequently carry outer vortex air into sunlit regions. These episodic conditions may be sufficient to produce a significant O₃ loss at 30 mbar during late November and December.

Diabatic cooling could bring this somewhat depleted air to ER-2 flight altitudes by early January. Summertime O₃ loss might also have some residual effect.

One of the striking results in the Antarctic campaign was the observed rapid decrease in O₃ and simultaneous increase in ClO as the aircraft crossed into the ozone hole along an isentropic flight leg¹⁰. On 9 February 1989, a similar but less dramatic isentropic O₃ decrease was observed poleward of the Arctic boundary⁴⁹ that was coincident with very high ClO and is shown in Fig. 4a, b. Figure 4a shows decreasing O₃ poleward of the vortex boundary that is collocated with decreasing N₂O. This positive correlation between O₃ and N₂O inside is contrasted by the usual negative correlation seen outside the boundary, implying O₃ loss within the vortex. Figure 4b shows no O₃ loss outside the boundary, substantial loss inside (implied by negative values for O₃ - O₃^{*}), and that the loss occurs precisely where ClO increases dramatically. Figure 4c demonstrates that this correlation between O₃ loss and ClO in the outer vortex persists throughout the mission and is evident even with constant N₂O. In this plot of all outer vortex data, ClO is the abscissa and O₃ - O₃^{*} the ordinate with Θ restricted to 435 ± 15 K. The data are tightly binned by N₂O value and each bin is provided with a linear fit. It is evident that O₃ loss and ClO are positively correlated over a wide range of N₂O, and the linear fits are surprisingly similar, although their slopes increase at the higher N₂O values.

Summary

Evaluating O₃ loss in the Arctic winter is complex because of our limited understanding of the effects of polar dynamics. Although there seems to be a consensus on significant diabatic cooling at high latitudes, and poleward flux into the Arctic vortex, there are uncertainties in the cooling rates and differing opinions on the altitude at which air is supplied to the vortex. Descent and poleward flux into the vortex (regardless of the altitude of the flux), along with concurrent O₃ loss together form a 'flowing processor', accepting air rich in O₃ from lower latitudes, and liberating air somewhat depleted in O₃ through the bottom of the vortex. The relative rates of O₃ loss and its resupply

determine whether a signature of that loss will be evident in isentropic and column analyses. To avoid these problems we have used a chemically conserved tracer, N₂O, to infer Arctic O₃ loss, a method similar to that used to infer loss in the exterior of the Antarctic ozone hole²⁷.

The analysis reveals an *in situ* O₃ loss of 500–1,500 p.p.b.v. (12–35%) throughout the vortex relative to its exterior. This corresponds to a decrease in column O₃ of about 6% over the 4 km depth covered in this analysis. If this loss is of anthropogenic origin emerging during the past decade, the decrease we report is consistent with the 4–10% long-term seasonal column change found by the Ozone Trends Panel²⁵. The rate of O₃ loss has been approximated by assuming vertical descent and a conservative cooling rate. Losses of 9–24 p.p.b.v. per day are obtained for parcels with N₂O from 210 p.p.b.v. to 130 p.p.b.v., respectively. These rates are comparable to but slightly higher than model calculations. Larger cooling rates and deviations from vertical descent will both increase this difference.

An O₃ loss was observed in early January that is too large to match model studies. The Arctic vortex polar asymmetry contrasts with the more symmetric Antarctic vortex, and the asymmetry could enhance early O₃ loss in the Arctic relative to the seasonally comparable period in the Antarctic. This would be due to episodic exposure to sunlight during the low-latitude excursions of the polar jet. The low values of O₃ found on 3 January indicate substantial O₃ loss before the mission and may result from this intermittent exposure.

We have found that the O₃ loss is correlated with elevated ClO in the outer vortex, along with enhancement of O₃ loss where there is maximum exposure of the vortex to sunlight. This suggests, but does not prove, that chlorine is an important factor in the ozone decrease. The agreement between this analysis and model studies is not perfect, particularly in early January. Perhaps alternative explanations of the data will emerge that do not require such large wintertime O₃ loss. In any case, it is clear that accurate evaluation of Arctic O₃ loss must account for the effects of polar dynamics. □

Received 21 December 1989; accepted 19 July 1990.

- Farman, J. C., Gardiner, B. G. & Shanklin, J. D. *Nature* **315**, 207–210 (1985).
- Hofmann, D. J., Harder, J. W., Rolf, S. R. & Rosen, J. R. *Nature* **326**, 59–62 (1987).
- de Zafra, R. L. *et al. Nature* **328**, 408–411 (1987).
- Solomon, S., Mount, G. H., Sanders, R. W. & Schmeltekop, A. L. *J. geophys. Res.* **92**, 8329–8338 (1987).
- J. geophys. Res.* **94**, Nos. D9 and D14 (1989).
- Proffitt, M. H. *et al. J. geophys. Res.* **94**, 16547–16555 (1989).
- Loewenstein, M., Podolske, J. R., Chan, K. R. & Strahan, S. E. *J. geophys. Res.* **94**, 11589–11598 (1989).
- Brune, W. H., Anderson, J. G. & Chan, K. R. *J. geophys. Res.* **94**, 16649–16663 (1989).
- Chan, K. R., Scott, S. G., Bui, T. P., Bowen, S. W. & Day, J. *J. geophys. Res.* **94**, 11573–11587 (1989).
- Proffitt *et al. J. geophys. Res.* **94**, 11437–11448 (1989).
- Anderson, J. G. *et al. J. geophys. Res.* **94**, 11480–11520 (1989).
- Jones, R. L. *et al. J. geophys. Res.* **94**, 11529–11558 (1989).
- Rodriguez, J. M. *et al. J. geophys. Res.* **94**, 16683–16703 (1989).
- Farman, J. C. *Phil Trans. R. Soc. B* **279**, 261–271 (1977).
- Juckes, M. N. & McIntyre, M. E. *Nature* **328**, 590–596 (1987).
- Hartmann, D. L. *et al. J. geophys. Res.* **94**, 16779–16795 (1989).
- Danielsen, E. F. & Houben, H. *Anthropogene Beeinflussung der Ozonschicht*, 191–242 (DECHEMA-Frankfurt am Main, 1988).
- Tuck, A. F. *J. geophys. Res.* **94**, 11687–11737 (1989).
- Proffitt, M. H. *et al. J. geophys. Res.* **94**, 16797–16813 (1989).
- Murphy, D. M. *et al. J. geophys. Res.* **94**, 11669–11685 (1989).
- Watterson, I. G. & Tuck, A. F. *J. geophys. Res.* **94**, 16511–16525 (1989).
- Cariolle, D., Lasserre-Bigorry, A. & Royer, J. F. *J. geophys. Res.* **95**, 1883–1898 (1990).
- Hofmann, D. J. *et al. Nature* **340**, 117–121 (1989).
- Evans, W. F. *J. geophys. Res. Lett.* **17**, 167–170 (1990).
- Ozone Trends Panel *Present State of Knowledge of the Upper Atmosphere, 1988*, NASA Ref. Publ. 1208 (Natn. Tech. Inf. Serv., Springfield, Virginia, 1989).
- Geophys. Res. Lett.* **17**, No. 4 (1990).
- Proffitt, M. H., Fahey, D. W., Kelly, K. K. & Tuck, A. F. *Nature* **342**, 233–237 (1989).
- Solomon, S., Garcia, R. R. & Stordal, F. *J. geophys. Res.* **90**, 12981–12989 (1985).

- Garcia, R. R. & Solomon, S. *J. geophys. Res.* **90**, 3850–3868 (1985).
- Brasseur, G. J. & Solomon, S. *Aeronomy of the Middle Atmosphere* 2nd Edn (Reidel, Dordrecht, 1986).
- Perilskii, L. M., Solomon, S. & London, J. *Planet Space Sci.* **37**, 1527–1538 (1989).
- Strahan, S. E. *et al. J. geophys. Res.* **94**, 16749–16756 (1989).
- Gunson, M. R. *et al. J. geophys. Res.* (in the press).
- Rosenfeld, J. E., Schoeberl, M. R., Lait, L. R. & Newman, P. A. *Geophys. Res. Lett.* **17**, 345–348 (1990).
- Schoeberl, M. R. *et al. Geophys. Res. Lett.* **17**, 469–472 (1990).
- Brewer, A. W. *Q. J. R. met. Soc.* **75**, 351–363 (1949).
- Dobson, G. M. G. *Proc. R. Soc. A* **236**, 187–193 (1956).
- Brewer, A. W. & Wilson, A. W. *Q. J. R. met. Soc.* **94**, 249–265 (1968).
- Dütsch, H. U. *Can. J. Chem.* **52**, 1491–1504 (1974).
- London, J. F., Bojkov, S., Oltmans, S. & Kelley, J. I. *Atlas of the Global Distribution of Total Ozone July 1957–June 1967* NCAR tech. Note 113 (NCAR, Boulder, 1976).
- Bojkov, R. D. & Rumen, D. *Met. Atmos. Phys.* **38**, 117–130 (1988).
- Ozone Data for the World, Atmospheric Environment Service* Vol. No. 3 30, 312–318 (Can. Atmos. Envir. Serv. & World Met. Org., Toronto, 1989).
- Leovy, C. B. *et al. J. Atmos. Sci.* **42**, 230–244 (1985).
- Kent, G. S., Trepte, C. R., Farrukh, U. H. & McCormick, M. P. *J. Atmos. Sci.* **42**, 1536–1551 (1985).
- Farman, J. C., Murgatroyd, R. J., Silnickas, A. M. & Thrush, B. A. *Q. J. R. met. Soc.* **111**, 1013–1028 (1985).
- Salawitch, R. J. *et al. Geophys. Res. Lett.* **17**, 561–564 (1990).
- McKenna, D. S. *et al. Geophys. Res. Lett.* **17**, 553–556 (1990).
- Brune, W. H., Toohay, D. W., Anderson, J. G. & Chan, K. R. *Geophys. Res. Lett.* **17**, 505–508 (1990).
- Browell, E. V. *et al. Geophys. Res. Lett.* **17**, 325–328 (1990).

ACKNOWLEDGEMENTS. We thank Ed Danielsen, Stuart McKeen, George Mount, Susan Solomon, Michael Trainer and Adrian Tuck for their helpful comments, William Brune and Darin Toohay for the use of the ClO data, Melanie Steinkamp and Cynthia Proffitt for their help in Stavanger, Ken Aikin for producing the figures, and the ER-2 pilots and ground crew.